Available online at www.sciencedirect.com
ScienceDirect
Solar Energy Materials & Solar Cells 92 (2008) 628–633
Solar Energy Materials and Solar Cells
www.elsevier.com/locate/solmat

Electrochromic properties of porous NiO thin films prepared by a chemical bath deposition

X.H. Xia[a], J.P. Tu[a,*], J. Zhang[a], X.L. Wang[a], W.K. Zhang[b], H. Huang[b]

[a]Department of Materials Science and Engineering, Zhejiang University, Hangzhou 310027, China
[b]College of Chemical Engineering and Materials Science, Zhejiang University of Technology, Hangzhou 310032, China

Received 30 December 2007; accepted 13 January 2008
Available online 7 March 2008

Abstract

Highly porous nickel oxide thin films were prepared on ITO glass by a simple chemical bath deposition (CBD) method in combination with a following heat-treatment process. XRD analysis revealed that the as-deposited precursor film contained β-$Ni(OH)_2$ and γ-NiOOH, and they changed to cubic polycrystalline NiO after annealing. The FTIR results showed presence of free hydroxyl ion and water in the NiO thin films. The electrochromic properties of NiO thin films were investigated in an aqueous alkaline electrolyte (1 M KOH) by means of transmittance, cyclic voltammetry (CV) and chronoamperometry (CA) measurements. The NiO thin film annealed at 300 °C exhibited a noticeable electrochromism and good memory effect. The coloration efficiency was calculated to be 42 $cm^2 C^{-1}$ at 550 nm, with a variation of transmittance up to 82%. The porous NiO thin films also showed good reaction kinetics with fast switching speed, and the coloration and bleaching time were 8 and 10 s, respectively.

Keywords: NiO; Porous film; Electrochromic properties; Chemical bath deposition

1. Introduction

Electrochromic materials are able to change the optical properties persistently and reversibly by an external voltage [1]. They have attracted much attention in recent years because of their low power consumption, high coloration efficiency (CE), and memory effect under open circuit condition [2,3]. Among these materials, NiO is an attractive material due to its high electrochromic efficiency, large dynamic range, good cyclic reversibility, and low material cost [4,5]. A variety of methods have been used to prepare electrochromic NiO films, such as vacuum evaporation [6], sputtering [7,8], chemical vapor deposition [9], electro-deposition process [10], pulsed laser deposition [11], spray pyrolysis [12], sol–gel process [13], and chemical bath deposition (CBD) [14,15], etc.

CBD of oxide films was first realized by Nagayama et al. [16] who used the technique to prepare SiO_2 films on silicon wafers. The method involves immersion of a substrate in an aqueous solution containing a precursor species. Then the desired oxide/hydroxide precipitates preferentially on the substrate surface, producing a conformal film. CBD is an advantageous technique due to its low cost, low temperature and also convenient for large-area deposition. However, there are only a few reports on the optical properties of NiO thin films prepared by CBD [17–19]. Ristova et al. [19] investigated the electrochromic properties of CBD NiO thin films. But the NiO thin films exhibited a CE with 24 $cm^2 C^{-1}$, which was lower than the value reported by Maruyama et al. [9].

The electro-deposition NiO films prepared by Wu et al. [20] showed a highly porous structure and exhibited high transmittance variation up to 80% at 550 nm. The porous structure is believed to be helpful to the enhancement of electrochromic performance. In this present work, NiO thin films with huge porosity were prepared by a CBD method. The electrochromic and electrochemical properties of porous NiO thin films were investigated.

*Corresponding author. Tel.: +86 571 87952573; fax: +86 571 87952856.
E-mail address: tujp@zju.edu.cn (J.P. Tu).

0927-0248/$ - see front matter © 2008 Elsevier B.V. All rights reserved.
doi:10.1016/j.solmat.2008.01.009

2. Experimental

Solution for CBD was obtained by mixing 80 ml of 1 M nickel sulfate, 60 ml of 0.25 M potassium persulfate, and 20 ml of aqueous ammonia (25–28%) in a 250 ml pyrex beaker at room temperature. Clean ITO glass substrates with $2.5 \times 2.5\,cm^2$ in sizes, masked with polyimide tape to prevent deposition on the nonconductive sides, were used in this work. The ITO samples, placed vertically in the freshly resulting solution, were kept at 20 °C for 20 min to deposit the precursor film. Then they were washed with deionized water. After removing the tape masks, the coated samples were dried at 75 °C and then were annealed at different temperatures (300, 350, and 400 °C) in air for 1.5 h. The thickness of the annealed films was approximately 480 nm, determined with an alpha-step 200 profilometry.

The powder from the as-deposited precursor film was analyzed by thermogravimetry (TG) and differential thermal analysis (DTA) under N_2 atmosphere at a heating rate of $10\,°C\,min^{-1}$ in a temperature range of 25–575 °C. The morphology and microstructure of the as-deposited and annealed films were characterized by a field emission scanning electron microscopy (FESEM, Hitachi S-4700), X-ray diffraction (XRD, Philips PC-APD with Cu Kα radiation), and Fourier transform infrared (FTIR) measurements (Perkin Elmer System 2000 FTIR interferometer).

The transmission spectra of NiO thin films in the fully colored and fully bleached states were measured over the range from 200 to 900 nm with a SHIMADZU UV-240 spectrophotometer. Each spectrum was recorded ex situ (after the samples taken out of the three-compartment system, instantly rinsed and wiped off from the remaining persistent water). The cyclic voltammetry (CV) and chronoamperometry (CA) measurements were carried out in a three-compartment system containing 1 M KOH as electrolyte, Hg/HgO as reference electrode and a Pt foil as counter-electrode. CV measurements of NiO films were performed using a CHI660B electrochemical workshop with a scanning rate of $10\,mV\,s^{-1}$ between 0 and 0.77 V at room temperature (25 ± 1 °C).

3. Results and discussion

Hydroxide precursor thin film was prepared using CBD. The chemical reactions may occur as follows [15]:

$$[Ni(H_2O)_{6-x}(NH_3)_x]^{2+} + 2OH^- \rightarrow Ni(OH)_2 + (6-x)\,H_2O + xNH_3, \quad (1)$$

$$2Ni(OH)_2 + S_2O_8{}^{2-} \rightarrow 2NiOOH + 2SO_4{}^{2-} + 2H^+. \quad (2)$$

The as-deposited precursor films were uniform in appearance and exhibited gray in color. After annealing, the films were nearly transparent and found to be strongly adhered to the ITO substrate. The SEM images of the as-deposited precursor and annealed films are shown in Fig. 1. The as-deposited precursor film has a porous structure (Fig. 1a). After annealing treatment at temperatures in the range of 300−400 °C, the morphologies of the films have hardly any change (Figs. 1b–d). It is observed that the annealed films have porous structure, which is similar to that reported by Wu et al. [20].

The XRD patterns of powders from the as-deposited precursor and annealed films on ITO substrate are presented in Fig. 2. All the peaks of pattern a in Fig. 2

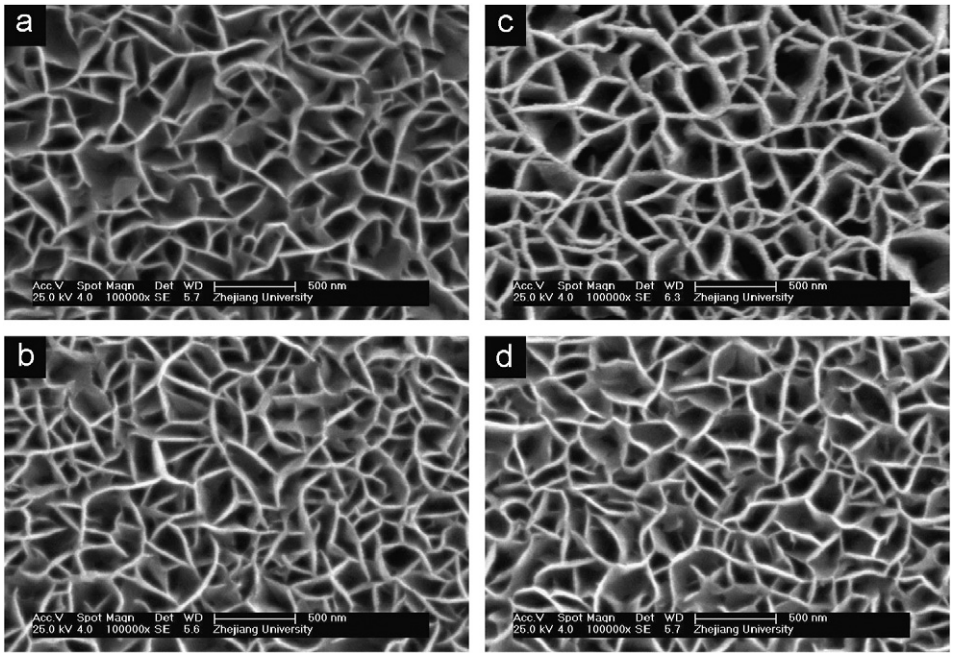

Fig. 1. SEM micrographs of (a) as-deposited precursor film and the films annealed at (b) 300 °C, (c) 350 °C, and (d) 400 °C.

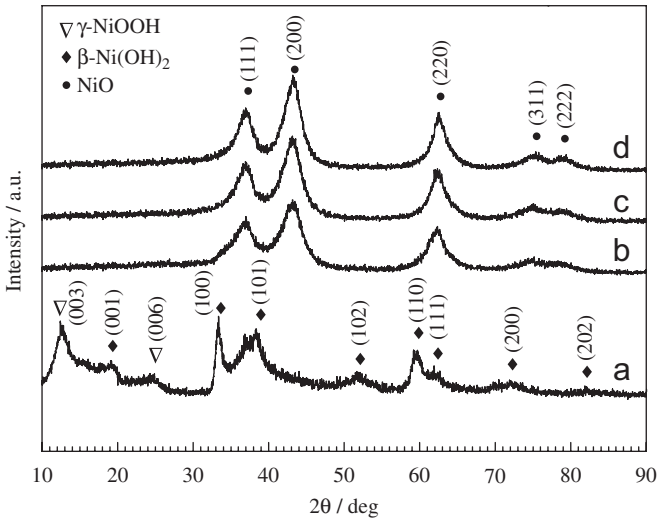

Fig. 2. XRD patterns of powders from (a) as-deposited precursor film and the films annealed at (b) 300 °C, (c) 350 °C, and (d) 400 °C.

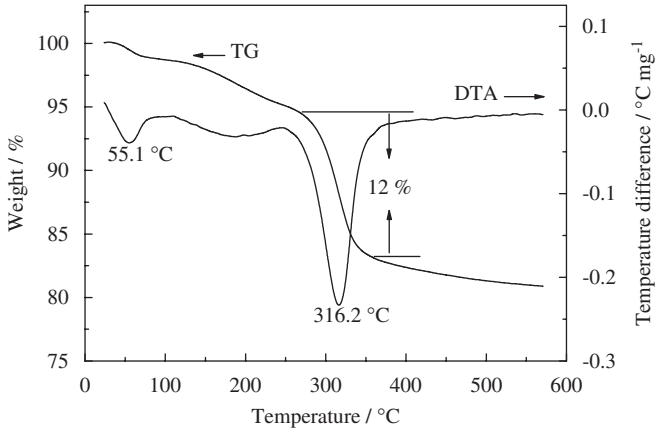

Fig. 3. TG–DTA curves of as-deposited precursor film.

indicate that the as-deposited precursor film contains β-$Ni(OH)_2$ (JCPDS 14-0117) and γ-NiOOH (JCPDS 06-0075). Han et al. [15] reported that the as-deposited films contained α-$Ni(OH)_2$ and $4Ni(OH)_2 \cdot NiOOH \cdot xH_2O$, while the work by Bukoves et al. [21] indicated that the as-deposited films contained $4Ni(OH)_2 \cdot NiOOH \cdot xH_2O$ instead of NiOOH or $Ni(OH)_2$. The difference is due to different preparing conditions, such as the reaction time, ageing time, reagent concentration, and reaction temperature. From patterns b–d in Fig. 2, the annealed films show diffraction peaks at 37.2°, 43.3°, 62.8°, 75.2°, and 79.4°, which correspond to (1 1 1), (2 0 0), (2 2 0), (3 1 1), and (2 2 2) crystal planes of cubic NiO phase (JCPDS 4-0835), respectively, indicating that polycrystalline NiO films have formed after heat treatment.

Typical TG and DTA curves of the as-deposited precursor film are shown in Fig. 3. The weight loss until temperature of 200 °C is attributable to dehydration of loosely bonded water. The acceleratory stage is in the temperature range of 275–350 °C in which the weight loss increases quickly to about 12%. In this temperature range, the DTA curve exhibits a dominant endothermic peak centered at 316 °C, which can be ascribed to the loss of water through decomposition of hydroxide prior to the formation of nickel oxide.

Fig. 4 shows the FTIR absorption spectra of powders from the films on ITO substrate. For the as-deposited precursor films, a sharp hydroxyl band centered at 3640 cm^{-1} corresponding to non-hydrogen bonds υ(OH) characteristic of β-$Ni(OH)_2$ phase [22] is presented in spectrum a of Fig. 4. A broad OH band centered 3420 cm^{-1} is indicative of hydrogen bonded water within the film structure and the band at 1650 cm^{-1} corresponds to the angular deformation of molecular water. The bands in the spectral region of 900–1150 cm^{-1} belong to sulphate groups (SO_4^{2-}) [23]. The bands at 526 and 459 cm^{-1} correspond to δ(OH) and υ(NiO) vibrations, respectively. It is clearly seen from Fig. 4

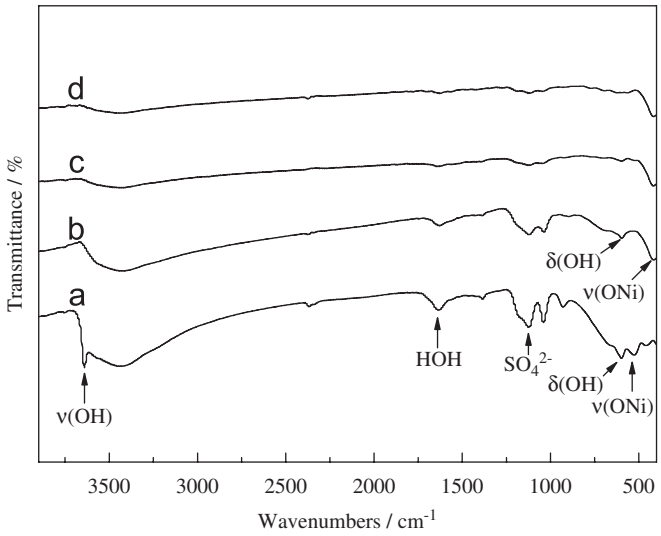

Fig. 4. The FTIR spectra of powders from (a) as-deposited precursor film and the films annealed at (b) 300 °C, (c) 350 °C, and (d) 400 °C.

that the phase has changed after heat treatment. For the film annealed at 300 °C, the sharp band at 3640 cm^{-1} disappears and a new strong band at 418 cm^{-1} corresponding to the stretching vibration of NiO [24] is observed in spectrum b of Fig. 4. Furthermore, the bands centered 3420, 1650, and 526 cm^{-1} in this spectrum indicates presence of free hydroxyl ion and water in the annealed films. From spectra c and d in Fig. 4, the peak intensities of free hydroxyl ion and water decrease with increasing the annealing temperature. It indicates that higher annealing temperature leads to better dehydration. The heating process removed most of the water and intercalated species, producing a hydrated nickel oxide film. Thus, both FTIR and XRD results are in complete agreement and show an effective formation of NiO.

The electrochromic properties of the NiO films were measured after the film electrodes had been subjected to cyclic voltammetric test for 10 cycles in KOH. The NiO film electrodes were colored by applying step voltages of 0.77 V for coloration and 0 V (vs. Hg/HgO) for bleaching.

The color of the NiO films changes from black (colored state) to transparent (bleached state). Fig. 5 shows spectral transmittance of the annealed NiO thin films in the colored and bleached states. It is clearly seen that the transmittance decreases as the annealing temperature increases. The NiO film annealed at 300 °C presents a noticeable electrochromism; the transmittance variation between colored and bleached states is high up to 82% at 550 nm. This is comparable with the result obtained by Wu et al. [20]. The transmittance variations of the films annealed at 350 and 400 °C are 51% and 31%, respectively. It is believed that higher heat-treatment temperature is favorable to the formation of compact crystalline nickel oxide [24]. The electrochromic process is associated with the double injection (extraction) of ions and electrons to (from) the film. A fully crystalline film is considered too dense for ion intercalation, and then it will result in low electrochromic performance. In addition, the loss of free hydroxyl ion and water in the NiO thin film may be also responsible for the degradation of electrochromic performance [25]. The hydroxyl ion and water play an important role in the electrochromic mechanism illustrated in CV investigation as below. As shown in the FTIR spectra (Fig. 4), the free hydroxyl ion and water exist in the NiO thin films. Moreover, the amount of hydroxyl ion and water decreases with increasing the annealing temperature. Therefore, an appropriate annealing temperature is at 300 °C in this work. The photographs of sample annealed at 300 °C in the colored and bleached states are shown in Fig. 6.

CE is defined as the ratio of change of optical density (ΔOD) of the film in its colored (T_c) and bleached (T_b) state at a certain wavelength and corresponding injected (or ejected) charge density (Q) per unit area. The change of optical density is obtained as follows:

$$\eta(\lambda) = \frac{\Delta OD(\lambda)}{Q}, \tag{3}$$

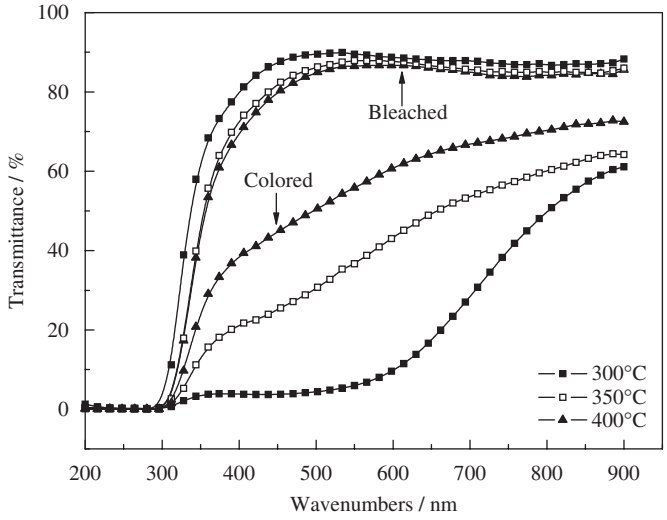

Fig. 5. Optical transmittance spectra of NiO thin films annealed at different temperatures.

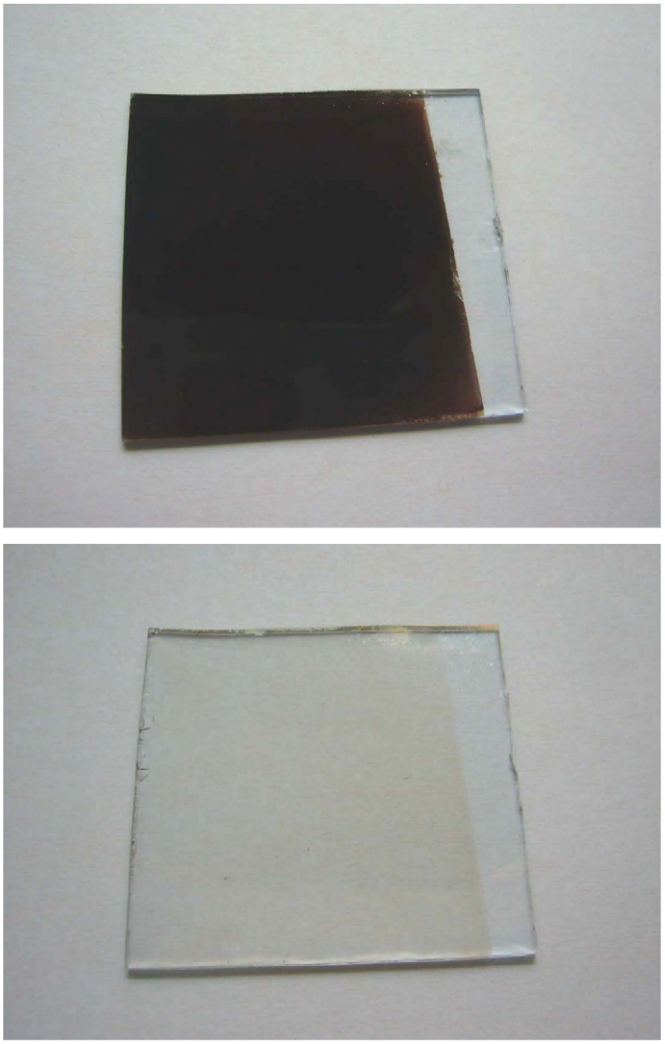

Fig. 6. Photographs of sample with a size of $2.5 \times 2.5\,cm^2$ in the colored and bleached states.

$$\Delta OD(\lambda) = \log \frac{T_b}{T_c}. \tag{4}$$

The general theory of electrochromism is in favor of that the amorphous structure gets higher value of CE because of its higher reactive surface, compared to the polycrystalline film. To the date the pure NiO reported with high CE are all amorphous films. In this work, the value of CE of the cubic polycrystalline NiO film annealed at 300 °C is calculated about $42\,cm^2\,C^{-1}$ at 550 nm. This value is comparable with those obtained from amorphous nickel oxide thin films grown by CVD ($44\,cm^2\,C^{-1}$) [9] and electro-deposition ($42\,cm^2\,C^{-1}$) [26], much higher than other films grown by CBD ($24\,cm^2\,C^{-1}$) [19], and other polycrystalline NiO thin films by laser pulsed deposition [27], spray pyrolysis [28], and sol–gel process [13]. This is mainly due to the highly porous structure. It has been pointed out that the coloration (bleaching) reaction is a double injection (extraction) of ions and electrons to (from) the film. The processes are believed to firstly occur at grain boundaries and on grain surfaces [29]. The highly porous

structure of NiO film provides large reaction surface and inner space. It also facilitates electrolyte soaking into the particles and shortens the proton diffusion paths within the bulk of NiO. Meanwhile, the intercrossing network provides much more paths for the double injection (extraction) of ions and electrons to (from) the film [20]. All these contribute to the improvement of electrochromic performance.

The electrochemical stability of the NiO thin film annealed at 300 °C was typically characterized by CV in the potential range of 0–0.77 V, at a sweep rate of 10 mV s^{-1}. The cycling life is based on essentially three processes consisting of an activation period (Fig. 7a), steady state (not shown), and a complex degradation period (Fig. 7b). Just one redox process is seen in the CV curve, which can be attributed to the following electrochemical reactions [30–32]:

$$NiO + OH^- \leftrightarrow NiOOH + e^- \quad (5)$$

or

$$NiO + H_2O \leftrightarrow NiOOH + H^+ + e^-,$$

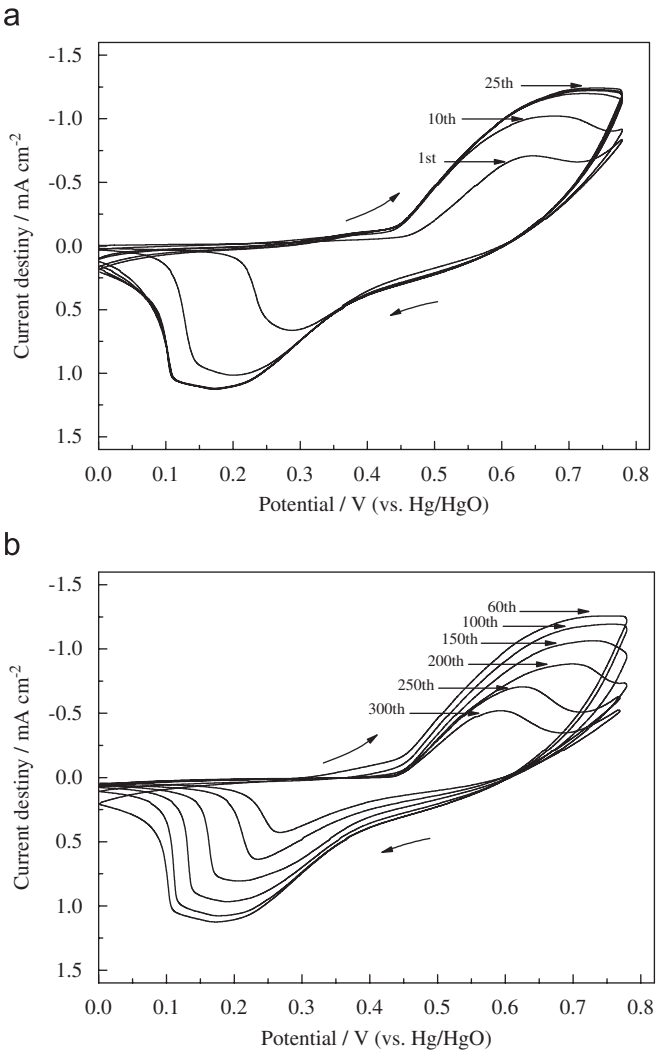

Fig. 7. Cyclic voltammograms of NiO thin film annealed at 300 °C.

and

$$Ni(OH)_2 \leftrightarrow NiOOH + H^+ + e^- \quad (6)$$

or

$$Ni(OH)_2 + OH^- \leftrightarrow NiOOH + H_2O + e^-.$$

The coloration process of the film is associated with the oxidation peak, whereas the bleaching process is associated with the reduction peak. Upon cycling, the film switches from brownish to transparent reversibly. The evolution of cyclic voltammograms in Fig. 7a suggests that the film nature and morphology are modified during the cycle. The oxidation and reduction peaks shift continuously to higher and lower potentials, respectively, leading to a larger potential separation between the oxidation and the reduction peak. The increase in anodic and cathodic current indicates that the amount of protons and electrons incorporated into the film increases with time, implying that the reaction activity of the NiO thin film increases with cycling. The intensity of the cathodic and anodic peaks increases up to the 25th cycle, then remains practically constant up to the 60th cycle, and finally starts to decrease. As the cycling is continued further (after 150 cycles), the anodic and cathodic peaks shift back to reverse directions. From Fig. 7b, it is noted that the current intensity decreases dramatically after the 100th cycle. The current intensity presents a fading of 6% at the 100th cycle, 16% at the 150th cycle, 30% at the 200th cycle, 43% at the 250th cycle, and 60% at the 300th cycle, respectively. Furthermore, parts of the film detach from the substrate after 300 cycles and the film electrode starts to break down. The cycling stability of the as-prepared film is inferior to that of films prepared by laser pulsed deposition [33] and sputtering [34].

In order to measure the stability of coloration, the NiO thin film was submitted to a memory test. The colored sample was left in air and the transmittance was measured at different intervals of time. Fig. 8 shows the evolution of the transmittance of NiO thin film after coloration. The NiO thin film annealed at 300 °C is colored at 0.77 V for 10 s to reach a transmittance of 5% at 550 nm. In an open circuit, the film starts to bleach to reach a transmittance value of about 6% and 9% after 12 and 24 h, respectively. This test shows that the annealed NiO film has a rather good memory effect.

The switching speed of NiO thin film from one state to another state is of great importance to determine its potential application. The time required for full bleaching from full colored state is defined as the response time. In this case, potentiostatic cycling was performed on the NiO thin film annealed at 300 °C between 0.77 and 0 V (vs. Hg/Hg). Fig. 9 shows the resultant current–time response. As the intercalation proceeds, the decrease in current with time is due to an increase in the chemical potential of the injected anions (OH^-) or cations (H^+). The response time for coloration is found to be about 8 s and for bleaching it is 10 s. The response time is dependent on

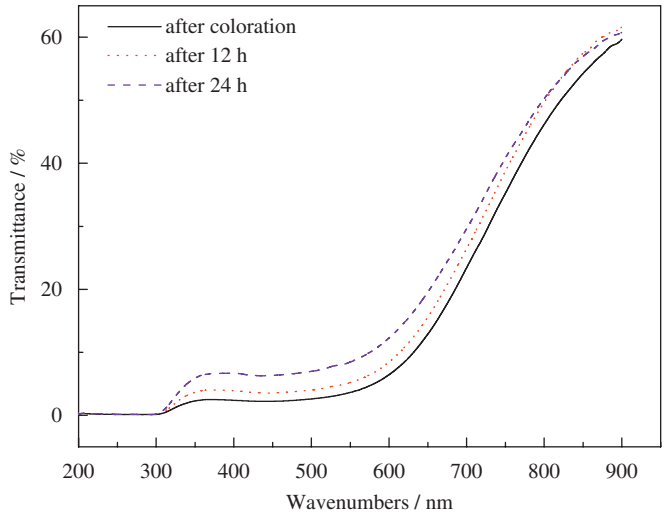

Fig. 8. Evolution of the transmittance of NiO thin film annealed at 300 °C after coloration.

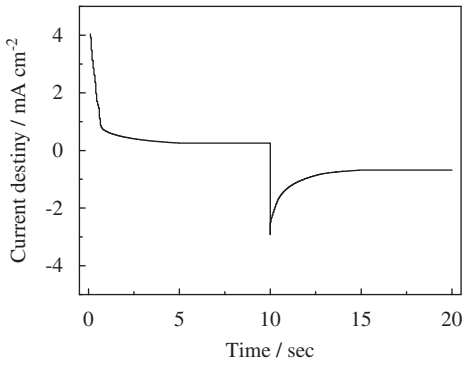

Fig. 9. Chronoamperometric curve of the electrochromic NiO thin film annealed at 300 °C.

several factors such as the applied potential, film thickness, and electrolyte conductivity. For the $Ni(OH)_2$ films prepared by electro-precipitation, the coloration and bleaching times were found to be about 20 and 40 s, respectively [35]. The NiO thin films prepared by spray pyrolysis technique need 15 and 20 s for coloration and bleaching, respectively [36]. In this work, the annealed NiO thin film has shorter response time, implying that it has better reaction kinetics. The highly porous structure of NiO thin film benefits electrolyte penetration and provides larger surface area for charge-transfer reactions.

4. Conclusion

Porous NiO thin films were prepared by a simple CBD at room temperature in combination with a following heat-treatment process. The as-deposited precursor film contained β-$Ni(OH)_2$ and γ-NiOOH, which converted to NiO after annealing treatment. The film annealed at 300 °C exhibited a rather good memory effect and a noticeable electrochromic performance with the variation of transmittance up to 82% and the high CE of 42 $cm^2 C^{-1}$ at 550 nm. In addition, the annealed NiO thin film showed good reaction kinetics with fast switching speed due to its highly porous structure. The coloration and bleaching time were 8 and 10 s, respectively.

References

[1] C.G. Granqvist, E. Avendano, A. Azens, Thin Solid Films 442 (2003) 201.
[2] C.G. Granqvist, J. Eur. Ceram. Soc. 25 (2005) 2907.
[3] C.G. Granqvist, Sol. Energy Mater. Sol. Cells 92 (2008) 203.
[4] C.G. Granqvist, Adv. Mater. 15 (2003) 1789.
[5] E. Avendano, L. Berggren, G.A. Niklasson, C.G. Granvist, A. Azens, Thin Solid Films 496 (2006) 30.
[6] J. Velevska, M. Ristova, Sol. Energy Mater. Sol. Cells 73 (2002) 131.
[7] A. Urbano, F.F. Ferreira, S.C. de Castro, R. Landers, M.C.A. Fantini, A. Gorenstein, Electrochim. Acta 46 (2001) 2269.
[8] J.L. Yang, Y.S. Lai, J.S. Chen, Thin Solid Films 488 (2005) 242.
[9] T. Maruyama, S. Arai, Sol. Energy Mater. Sol. Cells 30 (1993) 257.
[10] M.M. Uplane, S.H. Mujawar, A.I. Inamdar, P.S. Shinde, A.C. Sonavane, P.S. Patil, Appl. Surf. Sci. 253 (2007) 9365.
[11] N. Penin, A. Rougier, L. Laffont, P. Poizot, J.M. Tarascon, Sol. Energy Mater. Sol. Cells 90 (2006) 422.
[12] B.A. Reguig, M. Regragui, M. Morsli, A. Khelil, M. Addou, J.C. Bernede, Sol. Energy Mater. Sol. Cells 90 (2006) 1381.
[13] J.Y. Park, K.S. Ahn, Y.C. Nah, H.S. Shim, J. Sol–Gel Sci. Technol. 31 (2004) 323.
[14] B. Pejova, T. Kocareva, M. Najdoski, I. Grozdanov, Appl. Surf. Sci. 165 (2000) 271.
[15] S.Y. Han, D.H. Lee, Y.J. Chang, S.O. Ryu, T.J. Lee, C.H. Chang, J. Electrochem. Soc. 153 (2006) 382.
[16] H. Nagayama, H. Honda, H. Kawahara, J. Electrochem. Soc. 135 (1988) 2013.
[17] M.A. Vidales-Hurtado, A. Mendoza-Galvan, Mater. Chem. Phys. 107 (2008) 33.
[18] F.I. Ezema, A.B.C. Ekwealor, R.U. Osuji, J. Optoelectron. Adv. Mater. 9 (2007) 1898.
[19] M. Ristova, J. Velevska, M. Ristov, Sol. Energy Mater. Sol. Cells 71 (2002) 219.
[20] M.S. Wu, C.H. Yang, Appl. Phys. Lett. 91 (2007) 033109.
[21] P. Bukovec, N. Bukovec, B. Orel, K.S. Wissiak, J. Therm. Anal. 40 (1993) 1193.
[22] P. Oliva, J. Leonardi, J.F. Laurent, C. Delmas, J.J. Braconnier, M. Figlarz, F. Fievet, A. de Guibert, J. Power Sources 8 (1982) 229.
[23] A. Surca, B. Orel, B. Pihlar, P. Bukovec, J. Electroanal. Chem. 408 (1996) 83.
[24] R. Cerc Korošec, P. Bukovec, B. Pihlar, J. Padežnik Gomilšek, Thermochim. Acta 402 (2003) 57.
[25] H. Kamal, E.K. Elmaghraby, S.A. Ali, K. Abdel-Hady, Thin Solid Films 483 (2005) 330.
[26] S.A. Mahmoud, S.A. Aly, M. Abdel-Rahman, K. Abdel-Hady, Physica B 293 (2000) 125.
[27] L. Bouessay, A. Rougier, B. Beaudoin, J.B. Leriche, Appl. Surf. Sci. 186 (2002) 490.
[28] J. Arakaki, R. Reyes, M. Horn, W. Estrada, Sol. Energy Mater. Sol. Cells 37 (1995) 33.
[29] J. Nagai, Sol. Energy Mater. Sol. Cells 31 (1993) 291.
[30] S.I. Cordoba-Torressi, A. Hugot-Le Goff, S. Joiret, J. Electrochem. Soc. 138 (1991) 1554.
[31] M. Chigane, M. Ishikawa, J. Electrochem. Soc. 141 (1994) 3439.
[32] C. Natarajan, H. Matsumoto, G. Nogami, J. Electrochem. Soc. 114 (1997) 121.
[33] I. Bouessay, A. Rougier, P. Poizot, J. Moscovici, A. Michalowicz, J.M. Tarascon, Electrochim. Acta 50 (2005) 3737.
[34] Y. Ushio, A. Ishikawa, T. Niwa, Thin Solid Films 280 (1996) 233.
[35] M. Fantini, A. Groenstein, Sol. Energy Mater. 16 (1987) 487.
[36] L.D. Kadam, P.S. Patil, Sol. Energy Mater. Sol. Cells 69 (2001) 361.